

MATHEMATICAL MODEL FOR DEVELOPMENT AND OPTIMIZATION OF ULTRASONIC TRANSDUCERS FOR NON-DESTRUCTIVE TESTING IN THE NUCLEAR INDUSTRY

G. MAES

AIB-Vincotte, Koningslaan 157, 1060 Brussels, Belgium

Twin-crystal piezo-electric transducers are widely used for the ultrasonic inspection of austenitic material. The mathematical model, presented in this paper, is able to predict several important beam characteristics of such transducers. The model is based on the results of the far-field approximation of the Kirchhoff diffraction integral. Experimental measurements are compared to model predictions.

1 INTRODUCTION : ULTRASONIC NDT OF AUSTENITIC PRIMARY COMPONENTS

Because of their high mechanical strength and their resistance to corrosion, austenitic stainless steels are widely used in nuclear power plants. Most parts of the primary systems of both boiling water reactors (BWR) and pressurized water reactors (PWR), e.g. piping, pump casing (PWR), pressure vessel cladding, are commonly fabricated in austenitic material.

The most convenient technique for volumetric in-service inspection of pressurized components is ultrasonic testing, based on the propagation of high frequency (0.5 MHz to 10 MHz) elastic waves in the material, and the interaction of these waves with the material structure. An ultrasonic inspection method, most commonly used in non-destructive testing (NDT), the pulse-echo method, is shown schematically in fig.1. The elastic waves are generated and detected by a

probe containing a piezo-electric crystal. The electrical driving pulse, applied to the crystal, is transformed into a pressure wave which propagates into the material : at the given frequencies a sound beam is generated.

If the sound wave encounters a flaw in its path, part of the sound energy will be reflected back to the probe and the piezo-electric crystal will transform this energy into an electric signal, the flaw echo. Part of the ultrasonic beam usually by-passes the flaw and is reflected from the back wall of the test piece, yielding a back wall echo.

However, ultrasonic examination of austenitic steels, especially cast or welded components, is an extremely difficult matter. The elastic wave propagation is strongly affected by the coarse-grain structure of austenitic materials [1]. High, and variable attenuation of the signal, a poor signal-to-noise ratio (SNR), and deflection of the ultrasonic beam are the problems encountered. To overcome these difficulties, several new inspection techniques have been developed in the last two decades [2].

2 DEVELOPMENT OF DUAL-ELEMENT ANGLE BEAM TRANSDUCERS

For the ultrasonic inspection of coarse-grain materials, twin-crystal compression wave angle beam probes are the most widely used technique.

Such a transducer is shown schematically on fig.2. The apparent acoustic beam is produced by the intersection of the beams of the separate transmitter and receiver crystals. Thus, a quasi-focusing effect in the beam crossing re-

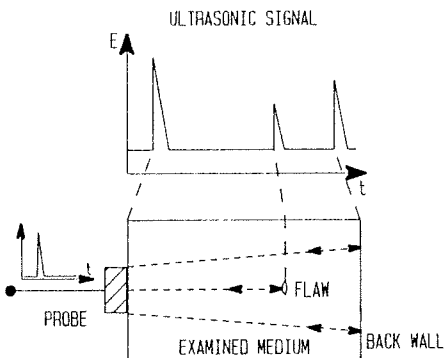


fig.1

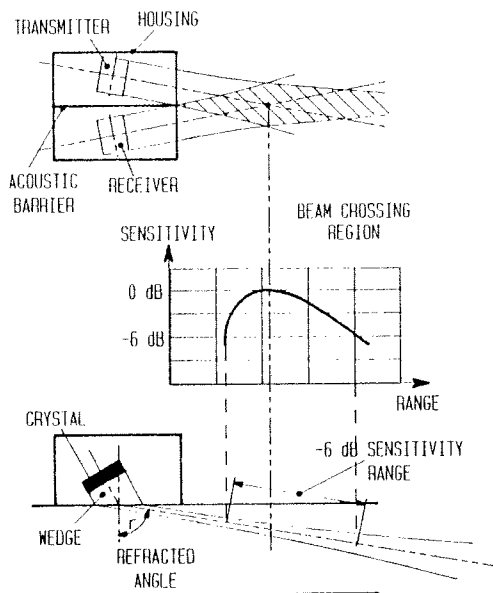


fig.2

gion is obtained, substantially improving the SNR of the ultrasonic signal. On the other hand, sufficient sensitivity is only provided over a limited depth range.

The probe designer has several options, to achieve focusing over the appropriate depth range. The plexiglass wedge determines the angle of the separate beams in the material, according to the laws of refraction. Changing either crystal dimensions or excitation frequency, will affect the shape of the beams.

Because of the variety of influencing parameters, the prediction of the resulting beam properties, e.g. beam diameter at -6dB, range of maximum sensitivity, is a rather complex matter. Thus, the development of a new type of transducer often involves the fabrication of several iterative prototypes, before the desired probe characteristics are obtained. This procedure is of course time-consuming and very costly.

A mathematical model for the twin-crystal transducer can contribute to both development and optimization, by offering rapid quantitative information about the influence of the variation of a parameter on the probe behaviour.

3 MATHEMATICAL MODEL FOR DUAL-ELEMENT ANGLE BEAM TRANSDUCERS

3.1 THEORETICAL PRINCIPLES :

The acoustic pressure distribution generated by

a rectangular piezo-electric crystal can be found by assuming a plane oscillator in an extended rigid wall, radiating into a perfect fluid (fig.3). For the moment, single-frequency toneburst excitation of the crystal is considered.

According to the Huygens principle, the acoustic pressure in a point $P(s,\alpha,\beta)$ is the result of the contributions of all elementary spherical wave sources on the oscillator. The Kirchhoff diffraction integral is the mathematical expression of this principle. From the results of the Fraunhofer approximation of the integral, valid in the far-field of the oscillator, a simple analytical expression is derived for the sound pressure p :

$$p(s,\alpha,\beta) = p_0 \cdot \frac{L \cdot B}{\lambda \cdot s} \cdot D(\alpha,\beta) \tag{1}$$

where p_0 is the sound pressure at the surface of the crystal, L , B are the dimensions of the crystal, λ is the acoustic wavelength, s the distance OP and α , β the angles giving the deviation of OP relative to the reference direction (normal to the crystal), as defined in fig.3.

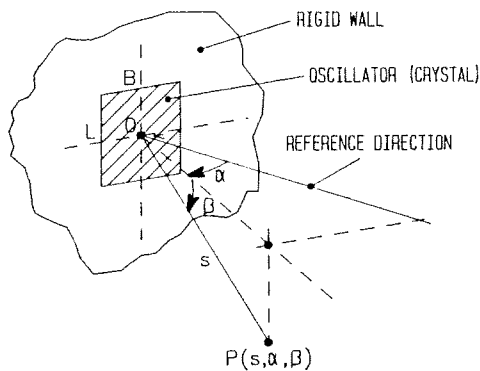


fig.3

The acoustic pressure decreases proportionally with $1/s$, which means that in its far-field the crystal can be considered as a point source, emitting spherical wavefronts. The angular dependency is given by the directivity function $D(\alpha,\beta)$, determined by the ratio of the crystal dimensions to the acoustic wavelength:

$$D(\alpha,\beta) = \text{sinc}\left(\frac{\pi \cdot B}{\lambda} \cdot \sin\alpha\right) \cdot \text{sinc}\left(\frac{\pi \cdot L}{\lambda} \cdot \sin\beta\right) \tag{2}$$

where $\text{sinc}(x) = \sin(x)/x$

To determine the acoustic pressure reflected from a target, it will be assumed for the mo-

ment, that the reflector subtends a small angle within the acoustic beam emitted from the crystal. This means that the variation of sound pressure over the surface of the reflector is negligible.

In fact, such a reflector will act as a secondary source of acoustic energy. Again assuming the far-field approximation, the reflected pressure distribution pF can be written as :

$$pF(s, \alpha, \beta) = p_{in} \cdot \frac{F}{s^n} \cdot DF(\alpha, \beta) \quad (3)$$

where p_{in} is the incoming sound pressure at the reflector surface and F is a parameter that depends on the reflector and theinsonified material. The power n , as well as the directivity function $DF(\alpha, \beta)$ depend on the type and the dimensions of the reflector. The reflector is supposed to be smooth and perfectly reflecting.

3.1.1 Acoustic field of a dual-element transducer :

To predict the beam dimensions and the focal range of a dual-element angle beam transducer, the normalised acoustic field amplitude of the transducer must be known. The acoustic field at a point P is the signal that would be received from a hypothetical infinitely small point reflector located in P . Such a reflector is a perfect source of spherical waves, showing no directional dependency. Thus, its acoustic pressure distribution is given by :

$$pF(s) \div p_{in} \cdot \frac{1}{s} \quad (4)$$

A twin-crystal probe can now be modelled as shown on fig.4. The point sources T and R , representing transmitter and receiver crystals, are virtual sources. Their positions in

the coordinate system, and their virtual dimensions, can be calculated from the real transducer design parameters.

The sound pressure distribution of the transmitter crystal is centred around a reference direction TK , which is the geometrical path of the ray originating in the centre of the actual crystal. Relative to this direction, the pressure distribution is described by an expression analogous to (1), yielding a sound pressure pT in P :

$$pT(sT, \alpha T, \beta T) = \frac{C}{sT} \cdot DT(\alpha T, \beta T) \quad (5)$$

where C is a constant.

The point P will reflect this pressure into a distribution given by (4). It is thus possible to calculate the sound pressure in R , the virtual location of the receiver crystal. However, the directivity function $DR(\alpha R, \beta R)$ of the receiver must also be taken into account, to determine the signal generated on the receiver. This function is given by a relation similar to (2), where RK is the reference direction. The final expression for the normalised acoustic field A , can be written as :

$$A(sT, sR, \alpha T, \alpha R, \beta T, \beta R) = \frac{N}{sT \cdot sR} \cdot DT(\alpha T, \beta T) \cdot DR(\alpha R, \beta R) \quad (6)$$

where N is the normalisation constant.

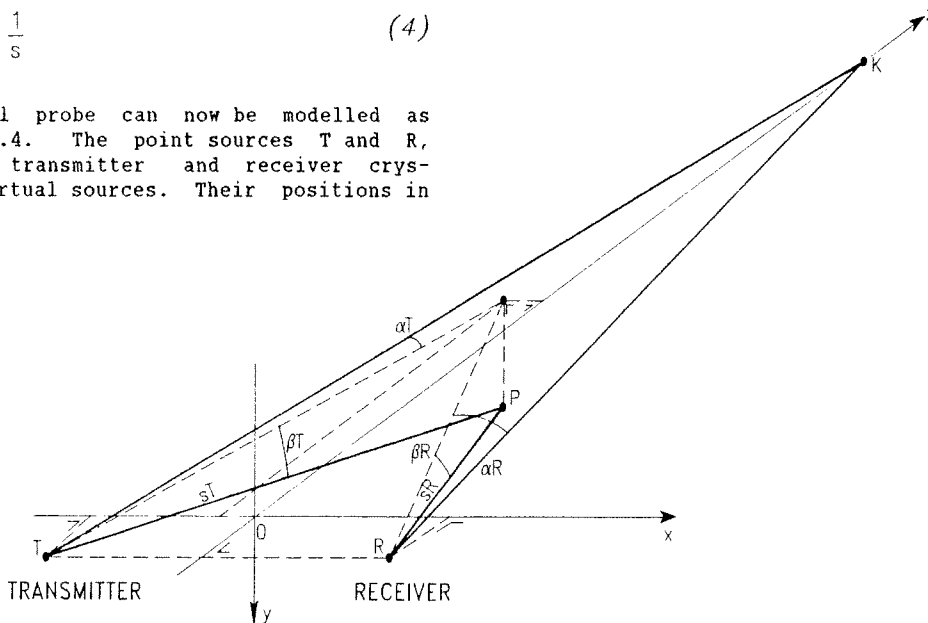


fig.4

3.1.2 Infinite flat reflector :

The secondary point source hypothesis, mentioned above, is not valid for the description of the interaction of a sound beam with an infinite flat reflector. In fact, whenever the reflector is considerably larger than the beam dimensions, it can be assumed to act like a mirror. Thus, it will reflect any incoming pressure distribution along the specular direction, without distortion.

Considering a flat reflector perpendicular to the nominal direction of the twin-crystal probe (direction OK of fig.4), the geometrical ray path TPR yielding an echo at the virtual receiver R, will inevitably be an isosceles triangle ($\alpha T = \alpha R$), lying in the TKR plane ($\beta T = \beta R = 0$). When transmitter and receiver crystals are identical, the echo amplitude can be predicted by :

$$E_{fl}(sT, \alpha T) = CP \cdot \frac{L \cdot B}{2\lambda \cdot sT} \left[\text{sinc} \left(\frac{\pi \cdot B}{\lambda} \cdot \sin \alpha T \right) \right]^2 \quad (7)$$

where CP is a constant, taking into account the piezo-electric properties of the crystals, i.e. the efficiency of the transformation of electrical into acoustical energy and vice versa. The variation of the reflection coefficient with the angle of incidence on the reflector is negligible.

It is clear that, for a given transducer configuration, the echo amplitude of an infinite flat reflector perpendicular to the nominal direction, only depends on the distance of the reflector.

3.1.3 Cylindrical reflector :

An infinitely long cylindrical reflector, with a diameter dc smaller than the beam dimension, will act as a secondary source of cylindrical waves. If a perfect line source is assumed, there is no directional dependency, and the reflected pressure distribution is given by :

$$pF(s) = p_{in} \cdot \sqrt{\frac{dc}{8 \cdot s}} \quad (8)$$

The echo amplitude for a cylindrical reflector of diameter dc , can then be predicted by :

$$E_{cyl}(sT, \alpha T) = CP \cdot \frac{L \cdot B}{2\lambda} \cdot \sqrt{\frac{dc}{2 \cdot sT}} \left[\text{sinc} \left(\frac{\pi \cdot B}{\lambda} \cdot \sin \alpha T \right) \right]^2 \quad (9)$$

or :

$$E_{cyl}(sT, \alpha T) = E_{fl} \cdot \sqrt{\frac{dc}{2 \cdot sT}} \quad (10)$$

relating the echo amplitudes of two reflectors commonly used in practice for calibration purposes.

3.1.4 Pulse excitation :

Up to now, a single-frequency toneburst excitation signal has been assumed for the piezoelectric crystal. However, in ultrasonic NDT mostly multiple-frequency or pulsed transducer activation is used.

In expression (7), giving the echo amplitude for an infinite flat reflector, the frequency f of the excitation signal doesn't appear. However :

$$f = \frac{V}{\lambda} \quad (11)$$

where V is the propagation velocity of the ultrasonic waves in the material. Substituting (11) in (7) yields an expression where f is explicitly present.

If the frequency domain transfer functions $T(f)$ and $R(f)$ of transmitter and receiver, and the spectrum $V(f)$ of the driving pulse are known, the extension to multiple-frequency activation can be done by integrating the contribution of each frequency, taking into account its appropriate phase [4]. Thus, the time dependent echo amplitude for an infinite flat reflector can be written as :

$$EP_{fl}(sT, \alpha T, t) = \int_{-\infty}^{+\infty} E(sT, \alpha T, f) \cdot \exp(2\pi i \cdot f \cdot t) df \quad (12)$$

$$E(sT, \alpha T, f) = \frac{L \cdot B}{2 \cdot V \cdot sT} \cdot f \cdot V(f) \cdot T(f) \cdot R(f) \cdot \left[\text{sinc} \left(\frac{\pi \cdot B}{V} \cdot f \cdot \sin \alpha T \right) \right]^2 \times \exp \left(-4\pi i \frac{f}{V} \cdot sT \right)$$

3.2 IMPLEMENTATION :

The analytical expressions derived in the preceding paragraphs, were implemented on commercially available, PC compatible software, offering simultaneously the basic tools and the flexibility needed for development purposes.

The first part of the program is an interface between the transducer design parameters, and the theoretical framework elaborated above. In a chosen coordinate system, positions and dimensions of the virtual sources simulating transmitter and receiver crystals, and the reference directions corresponding to the central rays are calculated, according to geometrical optics.

Next, the actual calculation of the resultant acoustic beam is performed, in the cartesian coordinate system of fig.4. For this purpose, the independent variables of equations (6), (7) or (9), $sT, sR, \alpha T, \alpha R, \beta T, \beta R$ are written as functions of the cartesian coordinates x, y, z .

3.3 VERIFICATION OF THE RESULTS :

All calculated results that are presented in this verification, were obtained assuming single-frequency toneburst excitation at the measured central frequency of the transducers.

Experimental data for the echo amplitude of an infinite flat reflector were obtained by standard probe characterisation measurements. The oblique face of a chamfered ferritic steel test block, chosen perpendicular to the ultrasonic beam, can be considered as an infinite flat reflector. As the probe is scanned over the surface of the block, the distance probe-reflector changes.

Fig.5 displays both experimental and calculated data for the normalised echo amplitude (sensitivity) of a 1 MHz, 45° transducer, as a function of the distance to the reflector. The qualitative similarity is obvious. The oscillations of the calculated amplitude are due to the single-frequency approximation.

Table I compares experimental and calculated results for the range of maximum sensitivity (RSM), and the extreme values of the -6dB sen-

TYPE	r (°)	EXPERIMENTAL DATA			CALCULATED DATA		
		RSM (mm)	R- (mm)	R+ (mm)	RSM (mm)	R- (mm)	R+ (mm)
V3315	42	33	15	135	23	12	70
V3316	45	54	20	135	43	25	100
V3326	45	74	37	150	52	33	105
V3534	45	21	11	47	15	8	32
V3540	59	14	7	34	11	6	27
V3541	70	10	5	26	3	2	9

table I

sitivity range (R-,R+). Calculated values for the RSM are typically 70 % of the measured values. The model gives a good approximation of the minimum R- of the -6dB range, while the maximum R+ is calculated at 70 % of the experimental value. At high refracted angles in the material, the calculated results deviate considerably from reality.

Detailed examination of the experimental data shows that the actual ultrasonic beams emerging from the piezo-electric crystals diverge less than predicted by the model. The geometrical approach for the calculation of the virtual dimensions of the point sources becomes less accurate with decreasing frequency and increasing angle. Table II displays the same quantities as table I, but in this case the virtual dimensions were deduced from experimental beam measurements. This yields calculated RSM values up to 90 % of the experimental measurements, but the -6dB sensitivity range is not enlarged.

TYPE	r (°)	EXPERIMENTAL DATA			CALCULATED DATA		
		RSM (mm)	R- (mm)	R+ (mm)	RSM (mm)	R- (mm)	R+ (mm)
V3315	42	33	15	135	31	17	85
V3316	45	54	20	135	49	30	105
V3326	45	74	37	150	57	37	112
V3534	45	21	11	47	16	10	32
V3540	59	14	7	34	13	8	27
V3541	70	10	5	26	4	2	10

table II

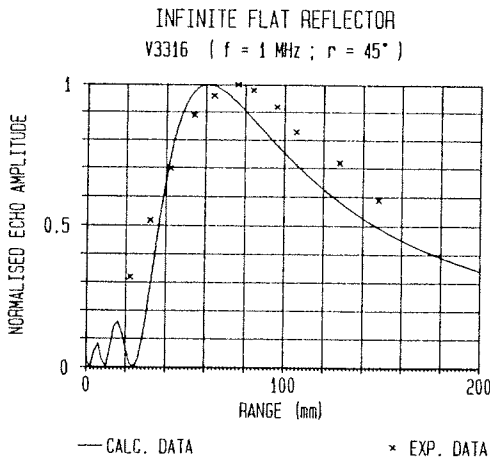


fig.5

Measurements of echo amplitude as a function of reflector distance were performed on 2 mm diameter side-drilled holes in a ferritic steel block. Both calculated (dimensions of virtual sources were deduced from beam measurements on single crystals) and experimental results are shown on figs.6-7 for a 1 MHz, 45° transducer, and a 2MHz, 60° transducer. As for the flat reflector, the calculated -6dB sensitivity range

is too short, but the RSM values are quite similar.

In both cases, the low values for the predicted sensitivity range might be due to the fact that the far-field approximation of expression (1) is less accurate for small values of s . A better approximation in this region could improve the quantitative results.

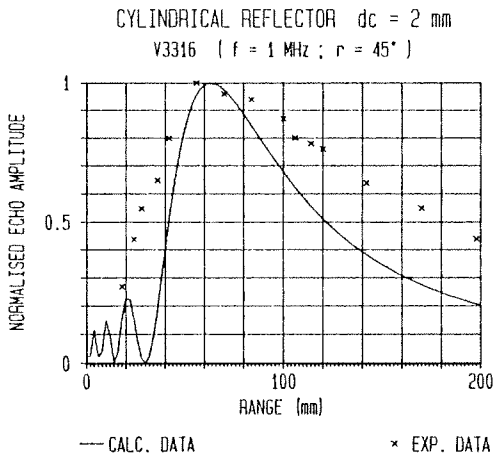


fig.6

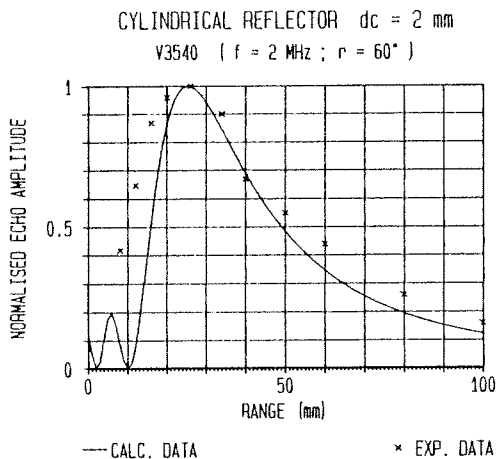


fig.7

4 CONCLUSIONS

A mathematical model was developed and implemented, describing the quasi-focusing effect of twin-crystal angle beam transducers.

Calculated data for the echo amplitudes of infinite flat reflectors and cylindrical holes were compared to experimental data for several types of transducers, commonly used in austenitic steel inspection practice. The agreement is promising, and optimization seems still possible.

5 REFERENCES

- [1] Silk, M.G, Ultrasonic Techniques for Inspecting Austenitic Welds, Research Techniques in NDT, Vol. IV (Academic Press, 1980).
- [2] Dombret, Ph. , Methodology for the Ultrasonic Testing of Austenitic Stainless Steel, SMIRT - 10 Post Conference Seminar n°3 on NDE in Relation to Structural Integrity, Monterey (CA), Aug. 1989.
- [3] Serabian S., An Assessment of the Detecting Ability of the Angle Beam Interrogation Method, Materials Evaluation, Dec. 1981, pp. 1243-49.
- [4] Serabian S., O'Callahan J.C., Pulsed Ultrasonic Flaw Detection Model, Materials Evaluation, June 1985, pp. 873-878.
- [5] Ermolov I.N., The Reflection of Ultrasonic Waves from Targets of Simple Geometry, Non-Destructive Testing, April 1972, pp. 87-91.
- [6] Krautkramer J., Krautkramer H., Ultrasonic Testing of Materials (Springer-Verlag 1977).